Random-field Ising model criticality in a glass-forming liquid

Benjamin Guiselin,[1,*] Ludovic Berthier,[1,2] and Gilles Tarjus[3]
[1]*Laboratoire Charles Coulomb (L2C), Université de Montpellier, CNRS, 34095 Montpellier, France*
[2]*Department of Chemistry, University of Cambridge, Cambridge CB2 1EW, United Kingdom*
[3]*LPTMC, CNRS-UMR 7600, Sorbonne Université, F-75005 Paris, France*

(Received 25 May 2020; accepted 7 October 2020; published 26 October 2020)

We use computer simulations to investigate the extended phase diagram of a supercooled liquid linearly coupled to a quenched reference configuration. An extensive finite-size scaling analysis demonstrates the existence of a random-field Ising model (RFIM) critical point and of a first-order transition line, in agreement with recent field-theoretical approaches. The dynamics in the vicinity of this critical point resembles the peculiar activated scaling of RFIM-like systems, and the overlap autocorrelation displays a logarithmic stretching. Our study demonstrates RFIM criticality in the thermodynamic limit for a three-dimensional supercooled liquid at equilibrium.

DOI: 10.1103/PhysRevE.102.042129

I. INTRODUCTION

What is the best starting point for a proper theoretical description of glass formation in supercooled liquids? The fact that this question remains hotly debated reflects the difficulty to provide a definite, and then widely accepted, resolution of the problem [1–3]. One strong candidate ascribes the slowing down of relaxation to properties of the free-energy landscape and to the presence of an underlying thermodynamic transition to an ideal glass phase [4]. This transition is unreachable, as it lies below the experimental glass transition T_g, but is nonetheless supposed to control glass formation in real materials. This theoretical approach, the random first-order transition (RFOT) theory [5], takes its strength from the exact analytical solution of glass-forming liquids in the limit of infinite dimensions of space, which realizes exactly the predicted scenario at a mean-field level [6,7]. Going from infinite to three dimensions (3D) is, however, a nontrivial qualitative leap, because spatial fluctuations are expected to play a key role and the very concepts of metastable states and free-energy landscape become ill defined.

What remains of the mean-field scenario in three dimensions? The dynamical (mode-coupling-like [8]) transition found at the mean-field level can at best survive as a crossover in finite dimensions [5,9,10], due to thermally activated processes, and its detection is always subject to interpretations. As for the putative RFOT at $T_K < T_g$, it is not directly testable, even with efficient swap Monte Carlo algorithms [11]. The mean-field or RFOT description puts the focus on an order parameter, the similarity or overlap between liquid configurations, and on its statistics. Following the well-established statistical mechanical formalism for phase transitions, one is then led to consider the role of specific boundary conditions and associated length scales [12] or, alternatively, of pinning fields and applied sources [13–15]. In this context, it is found that, at least at the mean-field level, applying a nonzero source ϵ linearly coupled to the overlap order parameter generates a line of first-order transition emanating from the RFOT at $(T_K, \epsilon = 0)$ and terminating in a critical point at a higher temperature $(T_c > T_K, \epsilon_c)$ [14,16]. Recent field-theoretical arguments beyond mean field [17,18] predict that this critical point should be in the universality class of the random-field Ising model (RFIM). The goal of the present work is to test whether this prediction is realized in a realistic three-dimensional glass-forming liquid [19]. Several previous attempts exist [16,20–24], but their conclusions have been mostly qualitative because of the impossibility to work at a low-enough temperature or because of much-too-small system sizes. We make here a qualitative decisive step forward by being able to study the proper range of temperatures as well as large system sizes (an order of magnitude larger than previous numerical investigations), allowing for an extensive finite-size study of the transition, which is the standard (but highly demanding) tool to analyze phase transitions. Furthermore, we characterize the nature of the slowing down of relaxation around the disordered critical point, which has never been done before. This allows us to establish, as well as possible using atomistic simulations, that the terminal critical point is in the universality class of the RFIM. Our work demonstrates that a nontrivial piece of the mean-field scenario is present in the phase diagram of finite-dimensional glass-forming liquids. This represents an additional physical application of the RFIM universality class, indeed an important topic for statistical mechanics studies of disordered systems.

II. METHODS

We consider a three-dimensional atomistic model glass-former that we study through state-of-the-art simulation techniques, including the recently developed swap algorithm [11,25] that allows us to equilibrate liquid configurations down to the conventional glass transition temperature T_g, umbrella sampling [26,27] and reweighting techniques [28] to

*benjamin.guiselin@umontpellier.fr

properly sample rare configurations, and isoconfigurational ensemble to obtain a better statistics for the dynamics [29]. We focus on the overlap between a configuration $\mathbf{r}^N = \{r^{(i)}, i = 1, \ldots, N\}$ of N atoms in equilibrium at temperature T and a quenched reference configuration $\mathbf{r}_0^N$ equilibrated at a temperature T_0: $\hat{Q}[\mathbf{r}^N; \mathbf{r}_0^N] = N^{-1} \sum_{i,j} w(|r^{(i)} - r_0^{(j)}|/a)$, where $w(x)$ is a strictly positive window function of width unity such that $w(0) = 1$, $w(+\infty) = 0$, and a is a small length accounting for thermal vibrations around the reference configuration.

Thermodynamic fluctuations are characterized by the free-energy cost to maintain the overlap $\hat{Q}$ at a given value Q,

$$V(Q|T; \mathbf{r}_0^N, T_0) = -\frac{T}{N} \ln \int d\mathbf{r}^N \frac{e^{-\beta \mathcal{H}[\mathbf{r}^N]}}{\mathcal{Z}(T)} \delta(\hat{Q}[\mathbf{r}^N; \mathbf{r}_0^N] - Q), \tag{1}$$

where $\beta = (k_B T)^{-1}$ (the Boltzmann constant is set to unity), $\mathcal{H}$ the liquid Hamiltonian, and $\mathcal{Z}(T)$ the partition function. This free energy is obtained from the probability distribution of the overlap $\mathcal{P}(Q|T; \mathbf{r}_0^N, T_0)$, which is the argument of the logarithm in Eq. (1). This is a random variable as it depends on the reference configuration $\mathbf{r}_0^N$, which is a source of quenched disorder. The average over $\mathbf{r}_0^N$ (taken with a Boltzmann distribution at temperature T_0) yields $V(Q|T; T_0) = \overline{V(Q|T; \mathbf{r}_0^N, T_0)}$, which is called the Franz-Parisi potential [14,16,30].

The dynamics near the critical point located at (T_c, ϵ_c) is investigated through the equilibrium overlap autocorrelation function,

$$C(t|\epsilon, T; \mathbf{r}_0^N, T_0) = \frac{\langle \delta\hat{Q}(t) \delta\hat{Q}(0) \rangle_\epsilon}{\langle \delta\hat{Q}(0)^2 \rangle_\epsilon}, \tag{2}$$

where $\delta\hat{Q} = \hat{Q} - \langle \hat{Q} \rangle_\epsilon$ and $\langle \cdot \rangle_\epsilon$ denotes a thermal average at temperature T in the presence of the applied source ϵ, such that the liquid Hamiltonian is now $\mathcal{H}_\epsilon[\mathbf{r}^N; \mathbf{r}_0^N] = \mathcal{H}[\mathbf{r}^N] - N\epsilon\hat{Q}[\mathbf{r}^N; \mathbf{r}_0^N]$. The above correlation function is again a random function, through the dependence on the reference configuration.

A severe obstacle that has hampered numerical studies of the putative critical point in the extended (T, ϵ) phase diagram is that when $T_0 = T$ the critical point is expected at a temperature T_c at which the relaxation time of the liquid is already so large that conventional simulation techniques are barely able to equilibrate the system at $\epsilon = 0$. We have solved this problem by using the swap algorithm that allows an equilibration of the continuously polydisperse liquid mixture under consideration (see the Supplemental Material [31]) much below what is attainable by standard methods [11,25]. To give an idea, present-day molecular dynamics simulations equilibrate the model down to $T \approx 0.1$, which is near the mode-coupling crossover ($T_{\rm mct} = 0.095$) whereas the swap algorithm allows equilibration down to $T \approx 0.055 < T_g$. To characterize the critical point we have therefore chosen a low temperature $T_0 = 0.06 \lesssim T_g$ for sampling the equilibrium reference configurations, which has the prime merit of significantly increasing the critical temperature $T_c(T_0)$ without altering its universality class [14,16–18]. We have also investigated whether the critical point persists when $T_0 = T$, and we provide strong evidence that it does.

We perform extensive computer simulations to study a wide range of system sizes, $N = 300$, 600, 1200, 2400 at number density $\rho = 1$. To perform the disorder average, we consider up to 28 different reference configurations. More details can be found in the Supplemental Material [31].

III. FINITE-SIZE SCALING ANALYSIS

We first present evidence for the presence of a transition line in the (T, ϵ) diagram separating a low-overlap from a high-overlap phase. Operationally, we use a method developed to study systems in the presence of quenched disorder when, contrary to the standard RFIM, there is no Z_2 inversion symmetry [44,45]. We compute the thermal susceptibility, $\chi_T(\epsilon, T; \mathbf{r}_0^N, T_0) = N\beta(\langle \hat{Q}^2 \rangle_\epsilon - \langle \hat{Q} \rangle_\epsilon^2)$, for each reference configuration $\mathbf{r}_0^N$ and temperature T, and we determine the location of its maximum, $\epsilon^*(T; \mathbf{r}_0^N, T_0)$. We next follow the evolution of the system along the disorder-averaged line $\epsilon^*(T; T_0) = \overline{\epsilon^*(T; \mathbf{r}_0^N, T_0)}$. The behavior of the probability distribution of the overlap along this line, $\mathcal{P}^*(Q|T; T_0) = \overline{\mathcal{P}(Q|\epsilon^*(T; T_0), T; \mathbf{r}_0^N, T_0)}$, is illustrated in Figs. 1(a) and 1(b). For a low-enough temperature [$T = 0.15$ in Fig. 1(a)] the probability is clearly bimodal and the width of the two well-separated peaks shrinks as N increases. The width of the low-overlap peak rescaled by the peak position follows the expected $N^{-1/2}$ behavior [46]. This is strong evidence for the presence of a first-order transition at low temperature when $N \to \infty$. The finite-size scaling (FSS) of additional quantities is provided in the Supplemental Material and supports as well the existence of a transition in the thermodynamic limit [31]. For higher temperatures [$T = 0.30$ in Fig. 1(b)], the probability distribution is bimodal for the smallest system sizes, but becomes single-peaked for the largest systems (hence the need to consider large system sizes and perform finite-size analysis to avoid considerably overestimating T_c). This region corresponds to a "Widom line" that is the locus of the (finite) maximum of the susceptibility. As one lowers the temperature along this line, one expects to cross a critical point at which the susceptibility diverges and below which a first-order transition is encountered, see Fig. 1(c). The overlap distributions at T_c evolve very much as the low-temperature ones in Fig. 1(a).

For RFIM-like systems without inversion symmetry, ratios of cumulants of the order parameter are not a practical way to detect the critical point [45]. Instead, to more precisely locate and characterize this critical point, we focus on the susceptibilities. Because of the quenched disorder associated with $\mathbf{r}_0^N$, and as in the case of the RFIM, one must consider two distinct susceptibilities, the connected one, $\chi_{\rm con}(\epsilon, T; T_0) = \overline{\chi_T(\epsilon, T; \mathbf{r}_0^N, T_0)}$, and the disconnected one, $\chi_{\rm dis}(\epsilon, T; T_0) = \beta N(\overline{\langle \hat{Q} \rangle_\epsilon^2} - \overline{\langle \hat{Q} \rangle_\epsilon}^2)$, which we evaluate at $\epsilon^*(T; T_0)$ for all temperatures and system sizes and then denote with a star. RFIM physics has a distinct signature in the behavior of these susceptibilities, because the disorder-induced fluctuations diverge much more strongly than thermal ones. As a result, for large but finite systems of linear size $L \propto N^{1/3}$ at the first-order transition and at the critical point [47]

$$\chi^*_{\rm dis}(T; T_0) \propto \chi^*_{\rm con}(T; T_0)^2. \tag{3}$$

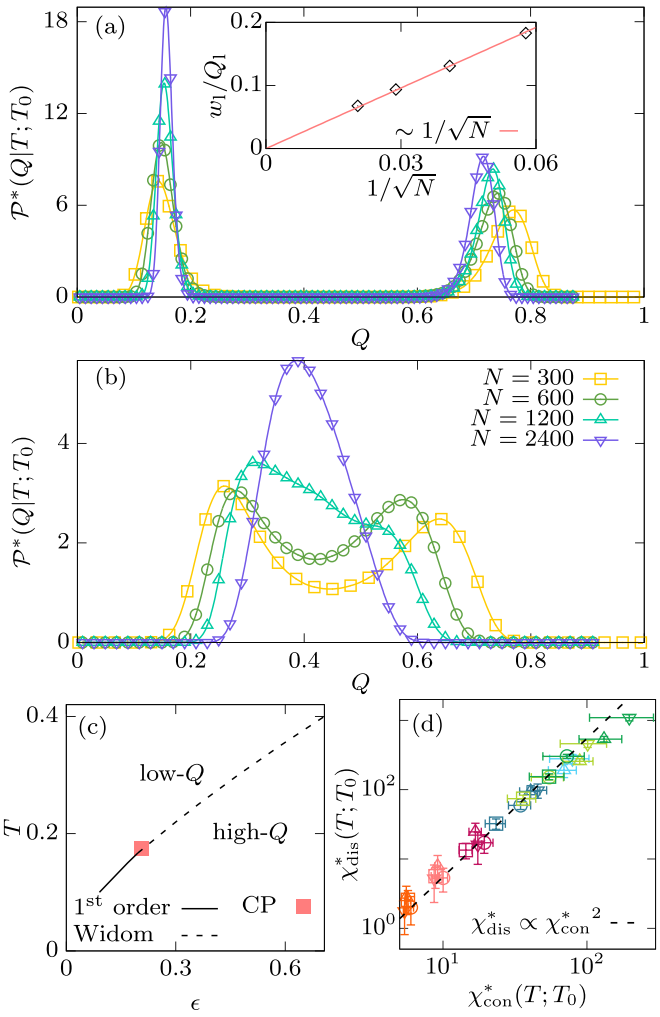

FIG. 1. [(a) and (b)] Overlap probability distribution $\mathcal{P}^*(Q|T;T_0)$ as a function of system size N below [$T = 0.15$ in (a)] and above [$T = 0.30$ in (b)] the critical point. The inset of (a) shows the half-width w_l of the low-overlap peak rescaled by the peak position Q_l as a function of $1/\sqrt{N}$. (c) (T, ϵ) phase diagram showing a first-order transition line at low temperature and a Widom line at high temperature, separated by a critical point (symbol). (d) Disconnected versus connected susceptibilities with a quadratic fit (dashed line); the symbols are as in panel (b), with the colors now denoting the different temperatures. Uncertainties are computed with the jacknife method [43].

This relation is very well obeyed by our data, as shown in Fig. 1(d). When approaching the critical point from above along the Widom line, the susceptibilities should follow the FSS behavior, i.e., $\chi^*_{con}(T;T_0) = L^{2-\eta}\widetilde{\chi}_{con}(tL^{1/\nu})$ and $\chi^*_{dis}(T;T_0) = L^{4-\bar{\eta}}\widetilde{\chi}_{dis}(tL^{1/\nu})$, where η, $\bar{\eta}$ and ν are critical exponents, $t = (T/T_c - 1)$ is the reduced temperature, and $\widetilde{\chi}_{con}(x)$ and $\widetilde{\chi}_{dis}(x)$ are scaling functions which are non-singular at $x = 0$. In Fig. 2 we display the outcome of our FSS analysis where we have used the known values of the critical exponents for the 3D RFIM: $\eta \approx 0.52$, $\bar{\eta} \approx 1.04$ and $\nu \approx 1.37$ [48]. The data collapse is excellent, with the critical point located at $T_c(T_0) \approx 0.167$ [which corresponds to $\epsilon_c(T_0) = \epsilon^*(T_c;T_0) \approx 0.20$] [51]. Hyperscaling violation also distinguishes the RFIM university class and implies that at

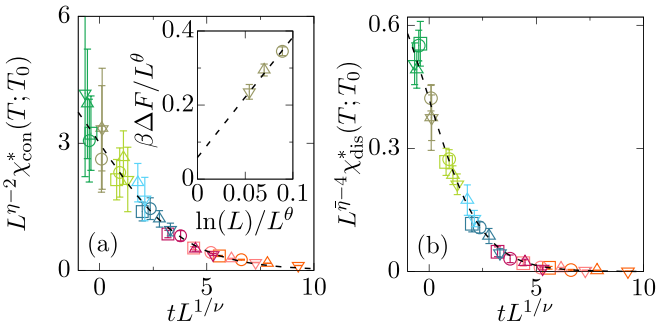

FIG. 2. (a) Connected susceptibility as a function of reduced temperature t rescaled according to the FSS ansatz with $\eta = 0.52$ and $\nu = 1.37$. Data from all sizes collapse onto a master curve $\widetilde{\chi}_{con}(x)$. The dashed line is a guide for the eye. (b) Equivalent plot for the disconnected susceptibility with $\bar{\eta} = 1.04$. In both panels, colors, and symbols are as in Fig. 1(d). Data in gray for $t \approx 0$ are obtained via a temperature reweighting from data at $T = 0.15$ [31]. The inset of panel (a) shows that the scaled free-energy barrier at the critical point $\beta\Delta F/L^\theta$ approaches a positive nonzero value as $L \to \infty$ with a $\ln(L)/L^\theta$ behavior, where $\theta = 1.49$.

the critical point the free-energy barrier ΔF between the low-overlap and the high-overlap phases is not scale invariant but instead grows as $\Delta F \sim \Upsilon L^\theta$, with $\theta \approx 1.49$ the temperature exponent [54] and Υ finite and nonzero. To extract ΔF, we measure the overlap distribution at $\epsilon^*(T;\mathbf{r}_0^N, T_0)$ for each individual sample. The inset of Fig. 2(a) shows that our data are compatible with a finite positive value of $\beta\Delta F/L^\theta \approx 0.08$ in the thermodynamic limit [55]. We provide additional FSS results in the Supplemental Material [31].

IV. CRITICAL DYNAMICS

We now turn to the study of the dynamics in the vicinity of the critical point, a study which has never been attempted before. Relaxation on approaching a critical point is characterized by a slowing down and a divergence of the relaxation time exactly at criticality. In the case of the RFIM, the slowing down is anomalous and described by an activated dynamic scaling according to which it is not the relaxation time $\tau(T)$ that grows as a power law of the correlation length $\xi(T)$, as usual, but its logarithm. In a renormalization-group framework this reflects the property that criticality is controlled by a zero-temperature fixed point [56,57]. From the correlation function of the overlap in Eq. (2) we define a relaxation time $\tau(\epsilon, T; \mathbf{r}_0^N, T_0)$ as the time at which $C(t|\epsilon, T; \mathbf{r}_0^N, T_0) = 0.2$. We approach the critical point from above and consider points (T, ϵ) at or close to the Widom line. Instead of the correlation length $\xi(T)$ to which we do not have direct access we use the connected susceptibility χ_{con} which scales as $\xi^{2-\eta}$. For the 3D RFIM, $2 - \eta \approx \theta$ and it has further been shown that $\psi = \theta$ [58] (so that $\xi^\psi \sim \chi_{con}$). We therefore consider the following form [59]:

$$\tau\left(\epsilon, T; \mathbf{r}_0^N, T_0\right) = \tau_0\left[\chi_T\left(\epsilon, T; \mathbf{r}_0^N, T_0\right)\right]^{z/\theta} e^{c\,\chi_T(\epsilon, T; \mathbf{r}_0^N, T_0)}, \quad (4)$$

with τ_0 and c some constants and z a dynamical exponent describing some subdominant behavior. Whereas the dominant activated scaling behavior is independent of the dynamics

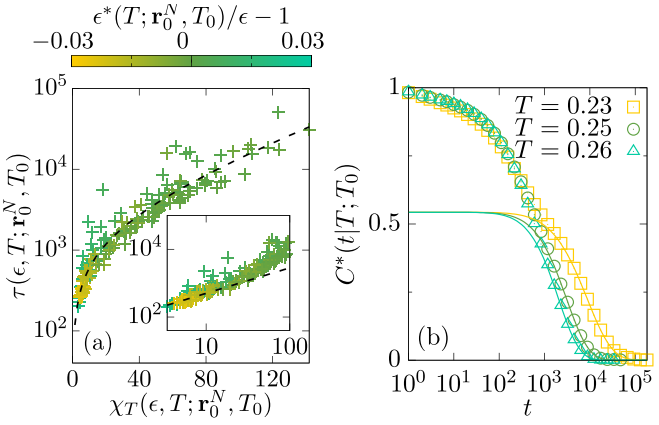

FIG. 3. (a) Relaxation time $\tau(\epsilon, T; \mathbf{r}_0^N, T_0)$ as a function of the thermal susceptibility $\chi_T(\epsilon, T; \mathbf{r}_0^N, T_0)$ for several samples $\mathbf{r}_0^N$, temperatures T, and sources ϵ. The color bar encodes the relative distance of the couple $(T,\ \epsilon)$ used for the simulation from $\epsilon^*(T; \mathbf{r}_0^N, T_0)$ in the ϵ direction. All data collapse on a master curve which is well fitted by Eq. (4) (dashed line), with $c = 0.015(2)$, $\tau_0 = 88(13)$ and $z = 1.15(10)$. The inset shows a tentative power-law fit which obviously fails at high values of the susceptibility. (b) Disorder-averaged overlap autocorrelation function along the Widom line for several temperatures. The full lines represent a fit to the empirical form presented in the main text, with $C_0 \approx 0.54$ and $\phi \approx 8.2$.

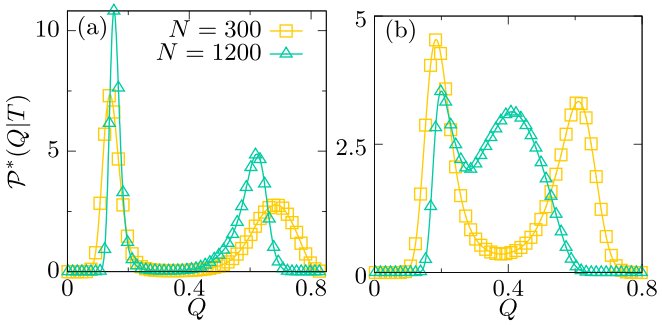

FIG. 4. Disorder-averaged overlap probability distribution below [$T = 0.085$ in (a)] and above [$T = 0.100$ in (b)] the critical point for the case $T_0 = T$.

(the overlap is in any case a nonconserved order parameter), the subdominant behavior and prefactors can be somehow modified by choosing an appropriate algorithm. Here, we consider the swap algorithm that is expected to speed up any pre-asymptotic dynamics. (We find that the ordinary Monte Carlo dynamics is much too slow near the critical point.) Figure 3(a) shows that the data agree well with the prediction in Eq. (4). The increase in relaxation time is limited to a little more than two orders of magnitude but it is sufficient to distinguish between activated scaling (main panel) and conventional power-law scaling (inset).

Another prediction of the activated dynamic scaling in the RFIM is that the correlation function should be very stretched, on a logarithmic scale, with $C(t;T) = \widetilde{C}(\ln t/\ln\tau(T))$ [57] and $\widetilde{C}(x)$ a scaling function for which no theoretical prediction is available. We find that along the Widom line, we can fit our autocorrelation data $C^*(t|T;T_0) = C(t|\epsilon, T; \mathbf{r}_0^N, T_0)$ with an empirical form previously used in RFIM-like systems [60–62], $\widetilde{C}(x) = C_0 \exp(-x^\phi)$, with C_0 and ϕ two T-independent adjustable parameters. As seen in Fig. 3(b), data at large times for all temperatures agree well with this prediction. A rescaling using the variable t/τ is instead inconsistent with the data. We stress that the activated critical slowing down that we analyze here in the vicinity of the critical point at $(T_c,\ \epsilon_c)$ is unrelated to the glassy slowdown of the bulk glass-former but requires the existence of a critical point in the RFIM universality class.

V. INFLUENCE OF THE TEMPERATURE OF THE REFERENCE CONFIGURATION

We finally come back to the issue of the persistence of a critical point when the temperature of the reference configuration is $T_0 = T$. This situation then probes typical states of the landscape and can be more directly related to the physics of a glass-forming liquid with no applied source. As already stressed, such study is computationally more demanding. We have therefore limited ourselves to checking the existence of a transition, without studying its nature in detail nor investigating the critical dynamics. The results are illustrated in Fig. 4 where we show the disorder-averaged overlap probability distribution $\mathcal{P}^*(Q|T)$. For $T = 0.085$ [in Fig. 4(a)], it becomes increasingly bimodal with N, the reduced half-width of the low overlap peak shrinking with N consistently with the existence of a first-order transition. By contrast, for $T = 0.100$ [in Fig. 4(b)], the probability function is bimodal at small N but the peaks rapidly approach each other as N increases, indicating that $\mathcal{P}^*(Q|T)$ should become single-peaked in the thermodynamic limit. Overall, our results suggest that the critical point also exists when $T_0 = T$, with $0.085 \leqslant T_c < 0.100$, close to or below the mode-coupling crossover, as eluded by past studies [22,24,63].

VI. CONCLUSIONS

To summarize, we have performed an extensive finite-size scaling analysis of a critical point proposed to characterize three-dimensional glass-formers, relying on the massive speedup afforded by the swap Monte Carlo algorithm combined with umbrella sampling techniques. Our results demonstrate for the first time the existence in the thermodynamic limit of a critical point, with a first-order transition line at lower temperatures, and our finite-size scaling analysis is consistent with the RFIM universality class in three dimensions. The critical point studied here is unique, since it represents, to date, the only piece of the mean-field or RFOT theoretical construction to survive other than as a crossover the introduction of finite-dimensional fluctuations. This closes, for three-dimensional liquids, a 25-year-old quest since its initial analysis in a fully mean-field context and more recent field-theoretical predictions, and gives us hope that a fundamental understanding of glass formation can be further developed in finite dimensions.

ACKNOWLEDGMENTS

We thank G. Biroli, C. Cammarota, D. Coslovich, M. Ediger, and R. Jack for fruitful discussions. Some simulations were performed at MESO@LR-Platform at the University of Montpellier. B. Guiselin acknowledges support by Capital Fund Management—Fondation pour la Recherche. This work was supported by a grant from the Simons Foundation (Grant No. 454933, L.B.).

[1] L. Berthier and G. Biroli, Rev. Mod. Phys. **83**, 587 (2011).
[2] G. Tarjus, *Dynamical Heterogeneities in Glasses, Colloids, and Granular Media*, International Series of Monographs on Physics, Vol. 150 (Oxford Science, Oxford, 2011), 39.
[3] D. Chandler and J. P. Garrahan, Annu. Rev. Phys. Chem. **61**, 191 (2010).
[4] V. Lubchenko and P. G. Wolynes, Annu. Rev. Phys. Chem. **58**, 235 (2007).
[5] T. R. Kirkpatrick, D. Thirumalai, and P. G. Wolynes, Phys. Rev. A **40**, 1045 (1989).
[6] J. Kurchan, G. Parisi, and F. Zamponi, J. Stat. Mech.: Theory Exp. (2012) P10012.
[7] G. Parisi, P. Urbani, and F. Zamponi, *Theory of Simple Glasses: Exact Solutions in Infinite Dimensions* (Cambridge University Press, Cambridge, UK, 2020).
[8] W. Götze, *Complex Dynamics of Glass-forming Liquids: A Mode-coupling Theory*, Vol. 143 (Oxford University Press, Oxford, 2008).
[9] V. Lubchenko and P. G. Wolynes, J. Chem. Phys. **119**, 9088 (2003).
[10] T. Rizzo, Europhys. Lett. **106**, 56003 (2014).
[11] A. Ninarello, L. Berthier, and D. Coslovich, Phys. Rev. X **7**, 021039 (2017).
[12] J.-P. Bouchaud and G. Biroli, J. Chem. Phys. **121**, 7347 (2004).
[13] R. Monasson, Phys. Rev. Lett. **75**, 2847 (1995).
[14] S. Franz and G. Parisi, Phys. Rev. Lett. **79**, 2486 (1997).
[15] C. Cammarota and G. Biroli, Proc. Natl. Acad. Sci. USA **109**, 8850 (2012).
[16] S. Franz and G. Parisi, Physica A **261**, 317 (1998).
[17] S. Franz and G. Parisi, J. Stat. Mech.: Theory Exp. (2013) P11012.
[18] G. Biroli, C. Cammarota, G. Tarjus, and M. Tarzia, Phys. Rev. Lett. **112**, 175701 (2014).
[19] Numerical and analytical arguments have previously been given for simple lattice (plaquette) glass models [64,65].
[20] M. Cardenas, S. Franz, and G. Parisi, J. Phys. A: Math. Gen. **31**, L163 (1998).
[21] M. Cardenas, S. Franz, and G. Parisi, J. Chem. Phys. **110**, 1726 (1999).
[22] C. Cammarota, A. Cavagna, I. Giardina, G. Gradenigo, T. S. Grigera, G. Parisi, and P. Verrocchio, Phys. Rev. Lett. **105**, 055703 (2010).
[23] L. Berthier, Phys. Rev. E **88**, 022313 (2013).
[24] L. Berthier and R. L. Jack, Phys. Rev. Lett. **114**, 205701 (2015).
[25] L. Berthier, E. Flenner, C. J. Fullerton, C. Scalliet, and M. Singh, J. Stat. Mech.: Theory Exp. (2019) 064004.
[26] G. M. Torrie and J. P. Valleau, J. Chem. Phys. **66**, 1402 (1977).
[27] D. Frenkel and B. Smit, *Understanding Molecular Simulation: From Algorithms to Applications*, Vol. 1 (Elsevier, Amsterdam, 2001).
[28] M. S. S. Challa and J. H. Hetherington, Phys. Rev. Lett. **60**, 77 (1988).
[29] A. Widmer-Cooper, P. Harrowell, and H. Fynewever, Phys. Rev. Lett. **93**, 135701 (2004).
[30] S. Franz and G. Parisi, J. Phys. I France **5**, 1401 (1995).
[31] See Supplemental Material at http://link.aps.org/supplemental/10.1103/PhysRevE.102.042129 for further practical details about simulations and more results related to finite-size scaling analysis, which includes Refs. [32–42].
[32] R. Gutiérrez, S. Karmakar, Y. G. Pollack, and I. Procaccia, Europhys. Lett. **111**, 56009 (2015).
[33] W. G. Hoover, Phys. Rev. A **31**, 1695 (1985).
[34] G. J. Martyna, M. E. Tuckerman, D. J. Tobias, and M. L. Klein, Mol. Phys. **87**, 1117 (1996).
[35] G. J. Martyna, M. L. Klein, and M. Tuckerman, J. Chem. Phys. **97**, 2635 (1992).
[36] M. P. Allen and D. J. Tildesley, *Computer Simulation of Liquids* (Oxford University Press, Oxford, 2017).
[37] M. Costeniuc, R. S. Ellis, H. Touchette, and B. Turkington, J. Stat. Phys. **119**, 1283 (2005).
[38] K. Hukushima and K. Nemoto, J. Phys. Soc. Jpn. **65**, 1604 (1996).
[39] L. A. Fernandez, V. Martín-Mayor, and D. Yllanes, Nucl. Phys. B **807**, 424 (2009).
[40] W. H. Press, S. A. Teukolsky, W. T. Vetterling, and B. P. Flannery, *Numerical Recipes 3rd Edition: The Art of Acientific Computing* (Cambridge University Press, Cambridge, UK, 2007).
[41] S. Wansleben and D. P. Landau, Phys. Rev. B **43**, 6006 (1991).
[42] R. B. Pearson, J. L. Richardson, and D. Toussaint, Phys. Rev. B **31**, 4472 (1985).
[43] M. Newman and G. Barkema, *Monte Carlo Methods in Statistical Physics* (Oxford University Press, Oxford, 1999).
[44] R. L. C. Vink, K. Binder, and H. Löwen, J. Phys.: Condens. Matter **20**, 404222 (2008).
[45] R. L. C. Vink, T. Fischer, and K. Binder, Phys. Rev. E **82**, 051134 (2010).
[46] K. Binder and D. P. Landau, Phys. Rev. B **30**, 1477 (1984).
[47] Strictly speaking, the relation is not exact at the critical point. In a RFIM-like system of linear size L, $\chi_{\rm dis} \sim L^{4-\bar{\eta}}$ and $\chi_{\rm con} \sim L^{2-\eta}$, with $\bar{\eta}$ and η the so-called anomalous dimensions. It turns out that for the 3D RFIM, $\bar{\eta} \approx 2\eta$, so that indeed to a very good approximation $\chi_{\rm dis} \propto {\chi_{\rm con}}^2$ [48–50].
[48] N. G. Fytas and V. Martín-Mayor, Phys. Rev. Lett. **110**, 227201 (2013).
[49] N. G. Fytas and V. Martín-Mayor, Phys. Rev. E **93**, 063308 (2016).
[50] G. Tarjus, I. Balog, and M. Tissier, Europhys. Lett. **103**, 61001 (2013).
[51] The best estimate of the critical temperature T_c is found by minimizing the average quadratic difference between the rescaled data and the master curve [52,53].
[52] J. Houdayer and A. K. Hartmann, Phys. Rev. B **70**, 014418 (2004).

[53] O. Melchert, arXiv:0910.5403.
[54] A. A. Middleton and D. S. Fisher, Phys. Rev. B **65**, 134411 (2002).
[55] K. Binder, Phys. Rev. A **25**, 1699 (1982).
[56] J. Villain, J. Phys. **46**, 1843 (1985).
[57] D. S. Fisher, Phys. Rev. Lett. **56**, 416 (1986).
[58] I. Balog and G. Tarjus, Phys. Rev. B **91**, 214201 (2015).
[59] Y. S. Parmar and J. K. Bhattacharjee, Phys. Rev. B **49**, 6350 (1994).
[60] A. T. Ogielski and D. A. Huse, Phys. Rev. Lett. **56**, 1298 (1986).
[61] S. B. Dierker and P. Wiltzius, Phys. Rev. Lett. **58**, 1865 (1987).
[62] R. Valiullin, S. Naumov, P. Galvosas, J. Kärger, H.-J. Woo, F. Porcheron, and P. A. Monson, Nature **443**, 965 (2006).
[63] L. Berthier, P. Charbonneau, D. Coslovich, A. Ninarello, M. Ozawa, and S. Yaida, Proc. Natl. Acad. Sci. USA **114**, 11356 (2017).
[64] R. L. Jack and J. P. Garrahan, Phys. Rev. Lett. **116**, 055702 (2016).
[65] G. Biroli, C. Rulquin, G. Tarjus, and M. Tarzia, SciPost Phys. **1**, 007 (2016).